Europe PMC Funders Group
Author Manuscript
Nat Cell Biol. Author manuscript; available in PMC 2017 January 03.

Published in final edited form as:
Nat Cell Biol. 2015 June ; 17(6): 771–781. doi:10.1038/ncb3167.

Condensin confers the longitudinal rigidity of chromosomes

Martin Houlard[1], **Jonathan Godwin**[1], **Jean Metson**[1], **Jibak Lee**[2], **Tatsuya Hirano**[3], and **Kim Nasmyth**[1,4]

[1]Department of Biochemistry, University of Oxford, South Parks Road, Oxford OX1 3QU, UK

[2]Laboratory of Developmental Biotechnology, Graduate School of Agricultural Science, Kobe University, 1-1 Rokkodai-cho, Nada-ku, Kobe 657-8501, Japan

[3]Chromosome Dynamics Laboratory, RIKEN, 2-1 Hirosawa, Wako, Saitama 351-0198, Japan

Abstract

In addition to inter-chromatid cohesion, mitotic and meiotic chromatids must have three physical properties: compaction into ‘threads’ roughly co-linear with their DNA sequence, intra-chromatid cohesion determining their rigidity, and a mechanism to promote sister chromatid disentanglement. A fundamental issue in chromosome biology is whether a single molecular process accounts for all three features. There is universal agreement that a pair of Smc–kleisin complexes called condensin I and II facilitate sister chromatid disentanglement, but whether they also confer thread formation or longitudinal rigidity is either controversial or has never been directly addressed respectively. We show here that condensin II (beta-kleisin) has an essential role in all three processes during meiosis I in mouse oocytes and that its function overlaps with that of condensin I (gamma-kleisin), which is otherwise redundant. Pre-assembled meiotic bivalents unravel when condensin is inactivated by TEV cleavage, proving that it actually holds chromatin fibres together.

There is no more fundamental or indeed marked transformation of chromatin fibres than that which precedes and facilitates their segregation during mitosis or meiosis. From occupying a broad and amorphous territory within the interphase nucleus1, individual DNA molecules metamorphose into thread-like sister chromatids2. Importantly, these chromatids possess sufficient plasticity along their longitudinal axes to prevent breakage of entangled sisters and yet enough rigidity to ensure that the chromatid is not unravelled when kinetochores are pulled towards the poles by microtubules. Remarkably, the segregation of most sister DNA sequences from each other (pre-segregation) takes place in the complete absence of spindle forces, facilitating sister chromatid disjunction at the onset of anaphase3. The metamorphosis of interphase chromatin into pre-segregated chromatids is known as chromosome condensation. However, this term does not adequately convey the reality that

[4]Correspondence should be addressed to K.N. (kim.nasmyth@bioch.ox.ac.uk).

Author Contributions

M.H. designed, performed and analysed the experiments. J.G. provided technical advice for oocytes manipulation. J.M. realized all the genotyping. J.L. provided reagents. T.H. provided reagents. K.N. designed and analysed the experiments and coordinated the work.

Competing Financial Interests

The authors declare no competing financial interests.

Europe PMC Funders Author Manuscripts
Europe PMC Funders Author Manuscripts

Europe PMC Funders Author Manuscripts

Europe PMC Funders Author Manuscripts

chromosome compaction generates threads not balls of chromatin. It also neglects the actuality that thread formation is accompanied both by pre-segregation and the generation of longitudinal rigidity4.

Cohesion holding sister DNAs together is mediated by a ring-shaped complex called cohesin, formed by the binding of the amino- and carboxy-terminal domains of an alpha-kleisin subunit5 to the ATPase heads at the vertices of V-shaped SMC1/SMC3 heterodimers. Pioneering work using *Xenopus* extracts showed that the metamorphosis of sperm chromatin into chromatids depends on condensins, cohesin-like ring complexes formed by the interconnection of ATPases at the vertices of SMC2/SMC4 heterodimers by either beta- (condensin II) or gamma- (condensin I) kleisins5–8. Whether condensin really drives thread formation has since been questioned. The most striking phenotype caused by condensin subunit mutations in fission yeast9,10, budding yeast11–13, worms14,15 and flies16,17 is the entanglement of sister chromatids during anaphase. Turning off transcription of *Smc2* in chicken cells has a similar effect18. The observation that thread formation, although sometimes delayed, still occurs in condensin mutants or in depleted cells has led to the suggestion that a factor other than condensin is in fact responsible for the compaction that creates threads per se19. Implicit in this proposal is that the dependence of thread formation on condensin in *Xenopus* extracts is either specific to this system and therefore not a universal feature or an artefact of the method used to inactivate the complex, namely immunodepletion. As the latter is difficult to reconcile with the fact that the depleted *Xenopus* extracts were rescued by purified condensin, an alternative possibility is that the genetic experiments are all flawed in so far as they failed fully to inactivate condensin.

Whether condensin is responsible for the longitudinal rigidity of chromatids has never been directly addressed. Nevertheless, the finding that sister kinetochores are pulled further apart than normal in condensin-depleted cells is consistent with the notion that condensin regulates the rigidity of chromatin fibres, at least in the vicinity of kinetochores20–22. To measure rigidity, it is necessary to measure a chromosome's extension when its two ends are pulled apart. This has been performed *in vitro* using either newt or even human chromosomes23. Such experiments have even hinted that chromatin associated with condensin might be more rigid than that associated merely with histones24 but have not directly addressed condensin's role in conferring rigidity.

Owing to the controversy surrounding condensin's role in thread formation and to address in particular its role in determining chromosome rigidity, we have used oocyte-specific transgenes in mice to induce deletion of floxed alleles of *Ncaph1* and *Ncaph2*, a technique that causes efficient depletion during both meiotic divisions of the gamma- and beta-kleisins associated with condensin I and II respectively. A great advantage of this system is that the extended prophase of oocytes causes severe protein depletion within a single cell cycle while co-orientation of maternal and paternal kinetochores during meiosis I ensures that spindle forces exert traction along chromatid axes (proximal to chiasmata) and not orthogonal to them as occurs during mitosis25, thereby revealing directly information about their longitudinal rigidity.

Europe PMC Funders Author Manuscripts

Europe PMC Funders Author Manuscripts

Results

Condensin II but not condensin I is essential for meiosis

To address condensin's role during meiosis, we used strains of mice containing floxed alleles of *Ncaph1*, encoding gamma-kleisin, and *Ncaph2*, encoding beta-kleisin. In both cases, deletion of the sequences flanked by LoxP sites generates frameshifts that truncate the proteins and eliminate C-terminal winged helical domains required for binding SMC4 (*Ncaph1*$^{\Delta}$ or *Ncaph2*$^{\Delta}$). To inactivate genes solely during meiosis in females, we used a transgene expressing Cre recombinase from the promoter region of the zona pellucida 3 gene (*Zp3Cre*), which induces deletion at the start of the oocyte's growing phase, two to three weeks before maturation26. Deletion efficiency was assessed by crossing heterozygous *flox/+Tg(Zp3Cre)* females to wild-type males. Genotyping of their progeny revealed 100% conversion of floxed alleles to deletions (Fig. 1a). Importantly, crosses between the resulting Δ/+ heterozygous mice never produced homozygous Δ/Δ offspring (Fig. 1a), implying that neither deleted allele can sustain development.

To address whether NCAPH1 or NCAPH2 is essential for meiosis, we analysed the fertility of *flox/flox Tg(Zp3Cre)* females by crossing them with wild-type males. This revealed that *Ncaph1* deletion by *Zp3Cre* had little or no effect whereas that of *Ncaph2* caused complete sterility (Fig. 1a). Identical results were obtained using a transgene expressing Cre recombinase from the *GDF9* promoter, which induces deletion earlier during oogenesis26 (three females *Ncaph1*$^{flox/flox}$ *Tg(Gdf9–iCre)* gave birth to two normal size litters each, all Δ/+). As *Ncaph1* deletion seems to cause an almost complete depletion of condensin's gamma-kleisin subunit (see below), the fertility of *Ncaph1*$^{flox/flox}$ *Tg(Zp3Cre)* females implies that NCAPH1 is unnecessary for either meiotic division or indeed the first zygotic division, during which there is apparently no transcription from the (wild-type) male pronucleus.

Oocytes are produced in normal quantities by *Ncaph2*$^{flox/flox}$ *Tg(Zp3Cre)* as well as *Ncaph1*$^{flox/flox}$ *Tg(Zp3Cre)* females. The latter underwent germinal vesicle breakdown (GVBD; Fig. 1b) and polar body extrusion (PBE) *in vitro* at rates similar to the wild type (Fig. 1c), although PBE was delayed by about one hour (Fig. 1d). In contrast, oocytes from *Ncaph2*$^{flox/flox}$ *Tg(Zp3Cre)* females underwent GVBD more slowly (Fig. 1b) and only 18% extruded a polar body (compared with 89% and 93% in *Ncaph1*$^{\Delta}$ and wild type respectively) and did so with a considerable delay (Fig. 1c,d). Interestingly, only 7.3% of *Ncaph2*$^{\Delta}$ oocytes underwent PBE when deletion was driven by *GDF9–iCre*, suggesting that earlier deletion might cause even more severe protein depletion (Fig. 1c). The lack of PBE in *Ncaph2*$^{flox/flox}$ *Tg(Zp3Cre)* oocytes was due to activation of the spindle assembly checkpoint (SAC), as injection of a messenger RNA encoding CDC20R132A, which cannot bind MAD2 (ref. 27), greatly increased the fraction of *Ncaph2*$^{flox/flox}$ *Tg(Zp3Cre)* oocytes that extruded polar bodies without improving chromosome segregation (Fig. 1e). These observations suggest that condensin II but not condensin I is indispensable for meiosis I.

Europe PMC Funders Author Manuscripts

Europe PMC Funders Author Manuscripts

Condensin II determines the morphology and rigidity of meiotic bivalents

To analyse the effects of inactivating condensin I and II on chromosome morphology in live oocytes, wild-type and mutant oocytes were injected at the GV stage with mRNA encoding mCherry-tagged H2B histone together with TALE-mClover_MajSat, which binds the major satellite repeat and thereby illuminates specifically pericentric chromatin28. Condensin I depletion had little or no effect on the metamorphosis of amorphous chromatin into thread-like bivalents (0.6 h post-GVBD), chromosome congression around the meiosis I spindle (3 h), bi-orientation on a metaphase plate (7 h), anaphase onset (9.5 h), or PBE (>10 h; Supplementary Fig. 1A and Supplementary Videos 1 and 2). We nevertheless noticed that chromosomes lacking condensin I were slightly shorter and rounder than the wild type, an effect that was more apparent in chromosome spreads (see below and Supplementary Fig. 1A). Despite this effect, depletion did not induce any noticeable stretching of pericentric chromatin either in metaphase I or metaphase II (Supplementary Video 2). Depletion of condensin II in contrast had a marked effect on chromosome morphology, which was noticeable at early (0.6 h) as well as late stages. Chromosomes were fatter and fuzzier. Stretching of pericentric sequences accompanied spindle attachment. Bi-orientation was greatly delayed but when it eventually took place, it was accompanied by a progressive distension of pericentric chromatin (Fig. 2 and Supplementary Videos 3 and 4). In rare oocytes that eventually manage to activate the APC/C and extrude polar bodies, the distension of pericentric chromatin is so extreme that spindle forces cannot effectively pull sister chromatids apart (Supplementary Fig. 1B), an effect that could be exacerbated by a failure also to disentangle them.

We also analysed the effects on chromosome morphology by spreading chromosomes at two different time points, namely 7 h post-GVBD when the bivalents are aligned on metaphase plates and in meiosis II following PBE. As previously reported29, both condensin complexes localize to the longitudinal axes of bivalents (meiosis I) and dyads (meiosis II). NCAPH1 was undetectable at this location in *Ncaph1*$^{flox/flox}$ *Tg(Zp3Cre)* oocytes (Fig. 3a), as was NCAPH2 in *Ncaph2*$^{flox/flox}$ *Tg(Zp3Cre)* oocytes, although a faint signal persisted at centromeres (Fig. 3b). Importantly, neither the distribution of NCAPH2 (Supplementary Fig. 2A) nor that of topoisomerase IIα (Supplementary Fig. 3A) was greatly altered by condensin I depletion, although DAPI staining showed that, when spread, bivalents were shorter and thicker and dyads less compact (Fig. 3a). Possibly owing to the swollen nature of chromatids and their lack of individualization, it is difficult to detect NCAPH1 or topoisomerase IIα along chromatid axes in oocytes lacking condensin II, although it remains readily detectable in the vicinity of centromeres (Supplementary Figs 2B and 3B).

Condensin is required for sister chromatid disentanglement even in the absence of cohesin

As a result of SAC activation, it is difficult to observe the phenotype most commonly observed in condensin-depleted cells, namely their failure to disentangle sister chromatids during anaphase. To circumvent this problem, we used *Rec8*$^{TEV/TEV}$ oocytes whose meiotic cohesin can be cleaved by the TEV protease30. In otherwise wild-type oocytes, injection of mRNA encoding TEV into *Rec8*$^{TEV/TEV}$ *Ncaph2*$^{f/f}$ oocytes, arrested in metaphase I by MAD2 overexpression31, triggers within 60 min complete disjunction of the four

Europe PMC Funders Author Manuscripts

Europe PMC Funders Author Manuscripts

chromatids normally held together in bivalents. The individual chromatids so produced then move back and forward on the meiosis I spindle, as previously described30 (Fig. 4a). In *Rec8*$^{TEV/TEV}$ *Ncaph2*$^{f/f}$ *Tg(ZP3Cre)* oocytes, on the other hand, much of the chromatin remains associated with a metaphase plate, implying defective chromatid disjunction.

As pericentric chromatin will have been extensively unravelled even before TEV injection in this experiment (see Fig. 2 right-most panel), the lack of disjunction could be caused as much by a lack of transmission of forces along the axes of chromatids as by an intrinsic (spindle-independent) defect in chromatid individualization (pre-segregation). We therefore repeated this experiment by injecting TEV protease at the GV stage, before any tension has been applied to pericentric chromatin by the spindle. The oocytes are then followed for 12 hours. This induced within the first nine hours post-GVBD efficient sister chromatid disjunction in *Rec8*$^{TEV/TEV}$ *Ncaph2*$^{f/f}$ but not in *Rec8*$^{TEV/TEV}$ *Ncaph2*$^{f/f}$ *Tg(ZP3Cre)* oocytes (Fig. 4b and Supplementary Videos 5 and 6). Thus, condensin II is necessary for sister chromatid disjunction even when pericentric chromatin has not been unravelled. Moreover, the lack of sister chromatid disjunction caused by condensin II depletion cannot be an indirect effect of failing to remove cohesin effectively32,33. Condensin II may be necessary for complete decatenation of sister DNAs by topoisomerase II (ref. 34).

Condensins I and II have overlapping functions

To address to what extent chromosome morphogenesis in the absence of condensin II is due to condensin I, we analysed the phenotype caused by simultaneous deletion of both *Ncaph1* and *Ncaph2*. To our surprise, *Ncaph1*$^{flox/flox}$ *Ncaph2*$^{flox/flox}$ *Tg(Zp3Cre)* oocytes activated the APC/C and extruded polar bodies with greater efficiency (63%) than *Ncaph2*$^{flox/flox}$ *Tg(Zp3Cre)* oocytes (18%). Nevertheless, both GVBD (Supplementary Fig. 4) and PBE (Fig. 5a) were delayed compared with wild-type controls. The restoration of PBE was not however due to any amelioration of chromosome morphology. On the contrary, morphologically distinguishable chromosomes were barely if at all detectable in spreads from *Ncaph1*$^{flox/flox}$ *Ncaph2*$^{flox/flox}$ *Tg(Zp3Cre)* oocytes (Fig. 5b). The higher frequency of PBE in the absence of both complexes presumably arises because chromosome disorganization is so pronounced that it stops the SAC functioning properly.

The massive disorganization of chromatin in doubly deleted oocytes was confirmed by live cell imaging (Fig. 5c,d and Supplementary Videos 7 and 8). The chromatin compaction and chromatid individualization that normally takes place 15 to 45 min after GVBD was largely absent. Although some chromatin eventually assembled into clumps that stretched along the spindle, pericentric sequences failed to coalesce into defined foci, and their stretching was more pronounced than in *Ncaph2*$^{flox/flox}$ *Tg(Zp3Cre)* oocytes (TALE-mClover_MajSat signal in Supplementary Video 8). Although chromatin masses associated with the two spindle poles, nothing remotely resembling chromosome segregation accompanied PBE. Two major conclusions can be drawn from this. First, although condensin I is redundant for meiosis I, chromosome formation in the absence of condensin II is largely driven by condensin I. In other words, the two complexes have overlapping functions. Second, it would seem that the formation of morphologically recognizable chromosomes cannot take place in the absence of both complexes.

Europe PMC Funders Author Manuscripts

Europe PMC Funders Author Manuscripts

Creation of a functional TEV-cleavable Ncaph2

Hitherto, almost all experiments addressing condensin's function have attempted to deplete subunits and then analyse the effect on chromatin metamorphosis accompanying entry into mitosis. Such experiments address condensin's role in building mitotic chromosomes but not its role in maintaining their structure. To do this, we tested the ability of mRNA encoding eGFP-tagged NCAPH2 containing TEV recognition sites (between amino acids 273/274) to restore chromosome segregation when injected into GV-stage *Ncaph2*$^{flox/flox}$ *Tg(Zp3Cre)* oocytes. PBE takes place later than in wild-type oocytes, possibly because condensin II is present and presumably active on GV-stage chromatin and it takes time for injected mRNAs to restore chromosome structure (Fig. 6a). Crucially, the eGFP-tagged TEV-cleavable protein enabled *Ncaph2*$^{flox/flox}$ *Tg(Zp3Cre)* oocytes to assemble normal-looking bivalents, localized like wild-type NCAPH2 along chromosome axes during meiosis I (Fig. 6b) and II (Supplementary Fig. 5), and restored normal congression, bi-orientation, and segregation during meiosis I. Co-injection of mRNAs encoding TEV protease abolished the association of NCAPH2 with chromosomes and prevented restoration of a normal morphology (Fig. 6b). Interestingly, injection of mRNAs encoding wild-type NCAPH2 into *Ncaph2*$^{flox/flox}$ *Tg(Zp3Cre)* oocytes arrested in metaphase I had little or no effect on their abnormal chromosome morphology (see below), suggesting that condensin II cannot fold up chromosomes that have been unravelled, at least in the presence of an active spindle apparatus.

Condensin maintains the morphology and rigidity of chromosomes

To address condensin's role in maintaining the structure of bivalents, we injected GV-stage *Ncaph2*$^{flox/flox}$ *Tg(Zp3Cre)* oocytes with mRNAs encoding MAD2 and either wild-type or TEV-cleavable eGFP-tagged NCAPH2 along with TALE-mClover_MajSat. The former prevented cells from activating the APC/C (ref. 31) and the latter rescued their morphological dysfunction. After bivalents had bi-oriented on metaphase plates, oocytes were injected for a second time, with mRNA encoding TEV protease (Fig. 7a). This had no effect in oocytes rescued with wild-type NCAPH2 (Fig. 7b, first panel and Supplementary Video 9) but caused rapid stretching of pericentric regions (marked by TALE-mClover_MajSat) as kinetochores moved to the spindle poles in those rescued by the TEV-cleavable version (Fig. 7b, second panel and Supplementary Video 10). Swelling and stretching of chromosome arms also occurred. Importantly, TEV converted the chromosomes within 60 to 100 min to a state resembling that found in unrescued oocytes, implying that it had completely destroyed condensin II function.

We repeated this experiment with *Ncaph1*$^{flox/flox}$ *Ncaph2*$^{flox/flox}$ *Tg(Zp3Cre)* oocytes. In this case, full rescue before TEV cleavage was rarely complete and as a consequence several bivalents failed to congress onto the metaphase plates (Fig. 7b, third panel and Supplementary Video 11). Nevertheless, TEV cleavage induced massive stretching of pericentric chromatin and dissolution of normal-looking bivalents as kinetochores moved to the spindle poles (Fig. 7b, bottom panel and Supplementary Video 12). These observations imply that condensin II actively maintains the rigidity of meiosis I bivalents along their longitudinal axes. In other words, it prevents their extension in response to spindle forces. Bivalents undergo modest extensions in length even in the wild type but these are invariably

Europe PMC Funders Author Manuscripts

Europe PMC Funders Author Manuscripts

transient, which is consistent with *in vitro* pulling experiments35. This elastic property seems to be destroyed by condensin cleavage.

During mitosis, kinetochore-based pulling forces are resisted not so much by the axes of chromosomes but by pericentric cohesion and the rigidity of chromatin fibres attaching kinetochores to the central constriction where this cohesion resides. To address whether condensin II is equally responsible for the rigidity (resistance to extension) of these fibres, we measured the effect of expressing TEV protease in meiosis II *Ncaph2*$^{flox/flox}$ *Tg(Zp3Cre)* oocytes that had undergone meiosis I following rescue with TEV-cleavable NCAPH2 (Fig. 8a). In contrast to meiosis I, condensin II cleavage during meiosis II caused only modest if any stretching of pericentric chromatin (wild-type Ncaph2: Supplementary Video 13; TEV-cleavable Ncaph2: Supplementary Video 14) and dyads remained on well-defined metaphase II plates (Fig. 8b). Despite its modest effects on chromosome morphology in live cells, TEV was clearly active under these circumstances as NCAPH2 was no longer associated with chromatid axes in chromosome spreads (Fig. 8c). This suggests that a factor other than condensin II is responsible for connecting kinetochores to the central constriction during meiosis II.

The stable association of condensin II with chromosomes

Pertinent to the mechanism by which condensin II prevents meiotic chromatids from unravelling when spindle forces are exerted along their longitudinal axes is whether the complex remains stably associated with chromatin or turns over rapidly, as is the case for condensin I during mitosis20. To address this, we photobleached one-half of the chromatin on metaphase plates following expression of eGFP-tagged NCAPH2 and its accumulation on bivalents and then measured the difference in fluorescence of bleached and unbleached halves at different points in time. This decreased with simple exponential kinetics, with a half-life of 2.4 h (Fig. 8d), implying that the entire population of condensin II associated with chromosomes turns over with a time constant of 0.29 h^{-1}. This means that less than 10% of chromosomal condensin II turns over during the interval it takes for bivalents to change from a normal to an extensively unravelled state on TEV injection (Supplementary Videos 10 and 12). The simplest explanation for this phenomenon is that TEV causes unravelling by removing condensin associated with chromatin and not merely by destroying the ability of complexes to associate *de novo*. In other words, by cleaving open the condensin ring, TEV seems to destroy a relatively stable structure holding together the bivalent's longitudinal axis. Consistent with this notion, wild-type eGFP-tagged NCAPH2 mRNAs failed to prevent unravelling when co-injected with TEV protease mRNAs (Supplementary Video 15). As injection with eGFP-tagged NCAPH1 mRNAs led to insufficient labelling of bivalents, we were unable to measure the dynamics of condensin I.

Discussion

Three features characterize the metamorphosis of interphase chromatin into mitotic chromosomes: formation of threads of compacted chromatin fibres, disentanglement of sister chromatid DNAs, and creation of longitudinal axes with the requisite rigidity. There are two new features of the approach we have used to address condensin's role in these

Europe PMC Funders Author Manuscripts

Europe PMC Funders Author Manuscripts

processes. First, we have used a method that can be guaranteed to inactivate the complex in a completely specific manner and at a defined stage of the cell cycle. By deleting floxed alleles of *Ncaph1* and *Ncaph2* using a transgene that is expressed during prophase two or three weeks before the first meiotic division, we managed to deplete either condensin I or condensin II from bivalent chromosomes and then observe the consequences as cells undergo the first meiotic division. Second, we replaced condensin II by an otherwise functional version that can be cleaved by TEV protease. This enabled us to observe for the first time the immediate consequences of removing condensin from pre-assembled chromosomes. Previous experiments in yeast have shown that condensin cleavage during metaphase causes problems with sister chromatid disentanglement during anaphase36 but did not address the role of condensin in maintaining chromosome structure during a defined state of the cell cycle such as metaphase. Our experiments leave no doubt that condensin is crucial not only for efficient sister chromatid disengagement, about which there has hitherto been universal agreement, but also for thread formation per se, which has been controversial, as well as conferring an axial rigidity capable of resisting spindle forces, which has not previously been addressed. Our finding that simultaneous depletion of condensins I and II has a marked effect on thread formation is consistent with previous findings using immunodepletion to explore condensin's function in *Xenopus* extracts7,37 and is hard to reconcile with the suggestion that 'chromosomes lacking condensin can condense and function in mitosis until the onset of anaphase'19.

We suggest that the robust thread formation observed in living cells when condensin was depleted using RNA interference32 or by turning off *Smc2* transcription18 arises because both sets of cells entered mitosis with amounts of condensin that still permitted thread formation but not efficient sister chromatid disentanglement. As some chromatin compaction still occurs in $Ncaph1^{flox/flox}$ $Ncaph2^{flox/flox}$ *Tg(Zp3Cre)* oocytes, we cannot at this juncture exclude the possibility that condensin-independent processes also contribute. In fact, our observation that PBE is less efficient in $Ncaph2^{flox/flox}$ *Tg(Gdf9–iCre)* than in $Ncaph2^{flox/flox}$ *Tg(Zp3Cre)* oocytes suggests that condensin II may not be completely depleted in the latter. Complete depletion might conceivably eliminate compaction altogether. It is interesting to note that our finding that condensins I and II have overlapping functions is consistent with observations that some eukaryotic organisms lack condensin II and others lack condensin I but none lack both38.

Our demonstration that condensin (be it I or II) is required for thread formation, disentanglement and rigidity raises a fundamental question, namely whether a single type of activity associated with condensin is capable of accounting for all three processes and if so what this might be. It has previously been pointed out that all three processes, as well as condensin's accumulation along chromatid axes, could be explained if the complexes were capable of attaching to small loops of chromatin in a manner that enabled such loops to enlarge in a processive manner, until adjacent condensin complexes at the base of such loops approached each other4. Such an activity would explain how condensin created a longitudinal axis whose integrity depended on that of the DNA, how DNA within loops would be segregated from their sisters, how sister inter-twining would be concentrated in intervals outside loops, between adjacent condensin complexes, which might create the

Europe PMC Funders Author Manuscripts

Europe PMC Funders Author Manuscripts

tension to drive decatenation by topoisomerase II, and last how the amorphous mass of chromatin in interphase is converted to threads (that is, chromosomes).

Condensin-like tripartite ring complexes are encoded by the genomes of most eu- and archaebacteria39 as well as all eukaryotes. Yet, the mechanism by which they function remains mysterious. Our finding that they confer and maintain axial rigidity constitutes an important advance, as this is a physiologically relevant parameter that actually can be measured *in vitro*35. Interestingly, it is a process that shares an important feature with cohesin, namely the holding of DNA segments together, be they from the same or different molecules. This insight was crucial in developing the notion that cohesin functions by entrapping DNAs inside its tripartite ring4, an idea that may have some traction also in the case of condensin40.

Methods

Mouse strains

Ncaph1$^{tm1a(EUCOMM)Wtsi}$ (MCEE; EPD0156_5_B09) and *Ncaph2*$^{tm1a(EUCOMM)Wtsi}$ (MBCH;EPD0070-2-G090) were obtained from the Wellcome Trust Sanger Institute. Both strains were first crossed with *Rosa–Flpe* mice to remove the β-galactosidase–neomycin reporter cassette to obtain the corresponding *flox* alleles. For *Ncaph1*, the *flox* sites are on both sides of exons ENSMUSE00000320721 and 00000320713. For *Ncaph2*, the *flox* sites are on both sides of exons ENSMUSE00000128853, 00000128862, 00000128849, 00000128847, 00000128846 and 00000128860. The *Ncaph1*$^{flox/+}$ and *Ncaph2*$^{flox/+}$ mice were then crossed with *Tg(Zp3Cre)* (or *Tg(GDF9–iCre)*) mice to obtain *Ncaph1*$^{flox/flox}$ *Tg(ZP3Cre)* or *Ncaph2*$^{flox/flox}$ *Tg(ZP3Cre)* experimental females. All experimental procedures were approved by the University of Oxford ethical review committee and licensed by the Home Office under the Animal (Scientific procedures) Act 1986. No statistical method was used to predetermine sample size. The experiments were not randomized. The investigators were not blinded to allocation during experiments and outcome assessment.

mRNA *in vitro* transcription

Ncaph2 cDNA (Origene, MC200537) was cloned in fusion at the 5′ end of the eGFP ORF in the pRNA vector. All of the following cDNAs were cloned in the pRNA plasmid and linearized by the indicated enzymes: Ncaph2–eGFP (AscI), H2B–mCherry (AscI), securin–eGFP (AscI), tubulin–eGFP (AscI), TEV protease (AscI) and Mad2 (SfiI). Linearized plasmids were then purified using the Zymoclean Gel DNA recovery kit (Zymo Research, Cat. D4002) and eluted using RNase free water (Ambion, AM9938). The cDNAs were then *in vitro* transcribed using the T3 mMESSAGE kit (Ambion). The TALE-mClover_MajSat (cloned in pTALYM9B15, Addgene) was linearized by NotI and transcribed using T7 mMESSAGE kit (Ambion). The *in vitro* transcribed RNAs were then purified using QUIAGEN RNeasy Minikit (Cat. 74104), eluted in RNase-free water. Aliquots were kept at −80 °C.

Europe PMC Funders Author Manuscripts

Europe PMC Funders Author Manuscripts

TEV-cleavable NCAPH2

Seven different TEV-cleavable versions of NCAPH2 were generated by inserting an AvrII site after the sequence corresponding to amino acids: 108, 188, 233, 273, 332, 409 and 493 using site-directed mutagenesis (Agilent) of pRNA–*Ncaph2–eGFP*. Three tandem TEV cleavage sites were then inserted in the AvrII site as previously reported41. The functionality of the different constructs was assessed by injecting the corresponding mRNA into oocytes lacking NCAPH2 and analysing by chromosome spreads 7 h post-GVBD both the loading of the protein and the chromosome shape. Only one version (TEV sites between amino acids 273 and 274) could be observed on the chromosomes and rescued their shape. This rescue was abolished by co-injection of TEV protease mRNA as represented in Fig. 6.

In vitro culture and oocytes micro-injection

Fully grown prophase-arrested GV oocytes were isolated from ovaries of females between 8 and 12 weeks old using sterile insulin needles in M2 medium (Sigma-Aldrich) supplemented with 200 μM IBMX (Sigma-Aldrich). mRNA micro-injection in the cytoplasm of oocytes was done as previously described30. Injected mRNAs (5–10 pl) were diluted in RNase-free water at the following concentrations: H2B–mCherry: 150 ng μl^{-1}, Mad2: 200 ng μl^{-1}, TALE-mClover_MajSat: 100 ng μl^{-1}, tubulin: 150 ng μl^{-1}, NCAPH2–eGFP: 50 ng μl^{-1}, TEV protease: 250 ng μl^{-1}. After injection, oocytes were incubated in M16+IBMX in a 5% CO_2, 37 °C incubator, to allow the full expression of the injected RNA. After washes in M16 to remove IBMX, oocytes were analysed by live cell confocal microscopy. Both M2 and M16 were prepared in water for embryo transfer (Sigma, W1503) according to the protocol and references indicated in ref. 42.

Live cell confocal imaging

Oocyte live cell imaging was done in 4-well Labtek chambers (ref. 155383) in 4 μl drops of M16 medium covered with mineral oil (Sigma) in a 5% CO_2 environmental microscope incubator at 37 °C (Pecon). Images were acquired using an LSM-780 confocal microscope (Zeiss) using the ZEN 2011 software. Between 7 and 12 slices (between 1 and 4 μm) were acquired every 5 to 15 min for each stage position using the autofocus tracking macro developed in J. Ellenberg's laboratory at EMBL (ref. 43). For detection of eGFP and mCherry, 488-nm and 561-nm excitation wavelengths and MBS 488/561 filters were used. Images were further analysed using Volocity software. For high-resolution videos, the lens used was a C-Apochromat ×63/1.20 W Corr UV–VIS–IR.

GVBD and PBE kinetics were done by injecting H2B–mCherry mRNA, and analysed using a lens Plan-Apochromat ×20/0.8 WD = 0.55 M27.

Securin degradation curves were realized as previously described44.

NCAPH2–eGFP photobleaching

GV-stage oocytes from *Ncaph2*$^{flox/flox}$ *Tg(ZP3Cre)* females were injected with H2B–mCherry-, Mad2- and NCAPH2–eGFP-coding mRNAs. After 16 h, oocytes arrested in meiosis I owing to MAD2 overexpression were transferred onto Labtek in M16 medium. Half the chromosome plate was photobleached using the ZEN 2011 bleaching tool on the

Europe PMC Funders Author Manuscripts

Europe PMC Funders Author Manuscripts

Zeiss 780 microscope: lens C-Apochromat ×63/1.20 W Corr UV–VIS–IR 7, zoom 3, 7 iterations of 70% 488 laser at scan speed 4. Images were then acquired just after bleaching and then every hour to prevent any bleaching during acquisition (12 *Z* stack, 1 μm apart using 2% 488 laser). Owing to partial mCherry bleaching during the photobleaching process, in the bleached region, the 561 laser detection gain was increased to detect the chromosome shape in both regions during data acquisition. After acquisition eGFP signal was quantified on the *Z*-projected images using ImageJ software. The chromosome surface corresponding to the bleached and non-bleached regions was defined according to the H2B–mCherry signal. The corresponding eGFP intensity for both areas was quantified and expressed as a ratio between bleached and non-bleached. Just after bleaching ($t = 0$) was defined as the maximum difference between the two (100%) and the recovery every hour as the percentage of the initial difference.

Chromosome spreading and immunostaining

After *in vitro* culture in M16 for the indicated time, oocytes were briefly incubated in M2 medium supplemented with 10 mg ml^{-1} Pronase (Sigma) at 37 °C to remove the zona pellucida, washed in M2 and incubated for 10 min in a hypotonic solution (50% SVF in deionized water) on agarose-covered plates. They were then fixed overnight in a humidified chamber at room temperature in a 10 μl drop of paraformaldehyde solution (1% paraformaldehyde, 0.15% Triton X-100, 3 mM dithiothreitol, adjusted to pH 9.2 with NaOH) in 15-well multichamber glass slide (MP Biomedicals). The morning after, the slides were dried, and briefly washed in 0.4% Photoflo/H_2O (Kodak). Slides were then washed for 5 min in PBS and then three times for 5 min in Spread Wash solution (PBS, 0.1% Tween20) supplemented with 0.2% BSA (Sigma). Each well of the slides was then covered (15 μl) in saturation solution (PBS, 0.1% Tween20, 2.5% BSA, 10% goat serum (DAKO)) and incubated for 1 h in a humidified chamber before incubation overnight with antibodies diluted in saturation solution: NCAPH1 (1:200; ref. 29), NCAPH2 (1:200; ref. 29), topoisomerase II alpha (Abcam, ab2987, 1:50), GFP (Abcam, ab290, 1:1,000). After three washes in PBS 0.1% Tween20, slides were incubated with the secondary antibody (Molecular Probes, 1/500) for 1 h. After three washes in PBS 0.1% Tween20, the slide were mounted in 30% Vectashield_DAPI in PBS (Vector) under a sealed coverslip.

Supplementary Material

Refer to Web version on PubMed Central for supplementary material.

Acknowledgements

We thank Micron microscopy facility and especially I. Dobbie for his technical support; all the staff of the BSB facility; B. Novák and all the members of the K.N. laboratory for discussions and comments on the manuscript. This work was supported by the Wellcome Trust (Grant Ref 091859/Z/10/Z), ERC grant (Proposal No 294401) and MRC (Grant ID 84673).

References

1. Cremer T, Tesin D, Hopman AH, Manuelidis L. Rapid interphase and metaphase assessment of specific chromosomal changes in neuroectodermal tumor cells by *in situ* hybridization with chemically modified DNA probes. Exp Cell Res. 1988; 176:199–220. [PubMed: 3288483]

Europe PMC Funders Author Manuscripts

2. Flemming W. Beitrage zur Kenntnisseder Zelle undIhreer Lebenserscheinungen. Archiv f mikrosk Anatomie. 1880; 18:151–259.
3. Nasmyth K. Segregating sister genomes: the molecular biology of chromosome separation. Science. 2002; 297:559–565. [PubMed: 12142526]
4. Nasmyth K. Disseminating the genome: joining, resolving, and separating sister chromatids during mitosis and meiosis. Annu Rev Genet. 2001; 35:673–745. [PubMed: 11700297]
5. Schleiffer A, et al. Kleisins: a superfamily of bacterial and eukaryotic SMC protein partners. Mol Cell. 2003; 11:571–575. [PubMed: 12667442]
6. Hirano T, Mitchison TJ. A heterodimeric coiled-coil protein required for mitotic chromosome condensation *in vitro*. Cell. 1994; 79:449–458. [PubMed: 7954811]
7. Hirano T, Kobayashi R, Hirano M. Condensins, chromosome condensation protein complexes containing XCAP-C, XCAP-E and a Xenopus homolog of the Drosophila Barren protein. Cell. 1997; 89:511–521. [PubMed: 9160743]
8. Ono T, et al. Differential contributions of condensin I and condensin II to mitotic chromosome architecture in vertebrate cells. Cell. 2003; 115:109–121. [PubMed: 14532007]
9. Saka Y, et al. Fission yeast cut3 and cut14, members of a ubiquitous protein family, are required for chromosome condensation and segregation in mitosis. EMBO J. 1994; 13:4938–4952. [PubMed: 7957061]
10. Sutani T, et al. Fission yeast condensin complex: essential roles of non-SMC subunits for condensation and Cdc2 phosphorylation of Cut3/SMC4. Genes Dev. 1999; 13:2271–2283. [PubMed: 10485849]
11. Strunnikov AV, Hogan E, Koshland D. SMC2, a Saccharomyces cerevisiae gene essential for chromosome segregation and condensation, defines a subgroup within the SMC family. Genes Dev. 1995; 9:587–599. [PubMed: 7698648]
12. Lavoie BD, Tuffo KM, Oh S, Koshland D, Holm C. Mitotic chromosome condensation requires Brn1p, the yeast homologue of Barren. Mol Biol Cell. 2000; 11:1293–1304. [PubMed: 10749930]
13. Bhalla N, Biggins S, Murray AW. Mutation of YCS4, a budding yeast condensin subunit, affects mitotic and nonmitotic chromosome behavior. Mol Biol Cell. 2002; 13:632–645. [PubMed: 11854418]
14. Lieb JD, Albrecht MR, Chuang PT, Meyer BJ. MIX-1: an essential component of the C. elegans mitotic machinery executes X chromosome dosage compensation. Cell. 1998; 92:265–277. [PubMed: 9458050]
15. Hagstrom KA, Holmes VF, Cozzarelli NR, Meyer BJ. C. elegans condensin promotes mitotic chromosome architecture, centromere organization, and sister chromatid segregation during mitosis and meiosis. Genes Dev. 2002; 16:729–742. [PubMed: 11914278]
16. Bhat MA, Philp AV, Glover DM, Bellen HJ. Chromatid segregation at anaphase requires the barren product, a novel chromosome-associated protein that interacts with Topoisomerase II. Cell. 1996; 87:1103–1114. [PubMed: 8978614]
17. Steffensen S, et al. A role for Drosophila SMC4 in the resolution of sister chromatids in mitosis. Curr Biol. 2001; 11:295–307. [PubMed: 11267866]
18. Hudson DF, Vagnarelli P, Gassmann R, Earnshaw WC. Condensin is required for nonhistone protein assembly and structural integrity of vertebrate mitotic chromosomes. Dev Cell. 2003; 5:323–336. [PubMed: 12919682]
19. Vagnarelli P, et al. Condensin and Repo-Man-PP1 co-operate in the regulation of chromosome architecture during mitosis. Nat Cell Biol. 2006; 8:1133–1142. [PubMed: 16998479]
20. Gerlich D, Hirota T, Koch B, Peters JM, Ellenberg J. Condensin I stabilizes chromosomes mechanically through a dynamic interaction in live cells. Curr Biol. 2006; 16:333–344. [PubMed: 16488867]
21. Ribeiro SA, et al. Condensin regulates the stiffness of vertebrate centromeres. Mol Biol Cell. 2009; 20:2371–2380. [PubMed: 19261808]
22. Oliveira RA, Coelho PA, Sunkel CE. The condensin I subunit Barren/CAP-H is essential for the structural integrity of centromeric heterochromatin during mitosis. Mol Cell Biol. 2005; 25:8971–8984. [PubMed: 16199875]

Europe PMC Funders Author Manuscripts

23. Poirier MG, Marko JF. Micromechanical studies of mitotic chromosomes. Curr Top Dev Biol. 2003; 55:75–141. [PubMed: 12959194]
24. Almagro S, Riveline D, Hirano T, Houchmandzadeh B, Dimitrov S. The mitotic chromosome is an assembly of rigid elastic axes organized by structural maintenance of chromosomes (SMC) proteins and surrounded by a soft chromatin envelope. J Biol Chem. 2004; 279:5118–5126. [PubMed: 14660618]
25. Nicklas RB. How cells get the right chromosomes. Science. 1997; 275:632–637. [PubMed: 9005842]
26. Lan ZJ, Xu X, Cooney AJ. Differential oocyte-specific expression of Cre recombinase activity in GDF-9-iCre, Zp3cre, and Msx2Cre transgenic mice. Biol Reprod. 2004; 71:1469–1474. [PubMed: 15215191]
27. Sironi L, et al. Mad2 binding to Mad1 and Cdc20, rather than oligomerization, is required for the spindle checkpoint. EMBO J. 2001; 20:6371–6382. [PubMed: 11707408]
28. Miyanari Y, Ziegler-Birling C, Torres-Padilla ME. Live visualization of chromatin dynamics with fluorescent TALEs. Nat Struct Mol Biol. 2013; 20:1321–1324. [PubMed: 24096363]
29. Lee J, Ogushi S, Saitou M, Hirano T. Condensins I and II are essential for construction of bivalent chromosomes in mouse oocytes. Mol Biol Cell. 2011; 22:3465–3477. [PubMed: 21795393]
30. Tachibana-Konwalski K, et al. Rec8-containing cohesin maintains bivalents without turnover during the growing phase of mouse oocytes. Genes Dev. 2010; 24:2505–2516. [PubMed: 20971813]
31. Wassmann K, Niault T, Maro B. Metaphase I arrest upon activation of the Mad2-dependent spindle checkpoint in mouse oocytes. Curr Biol. 2003; 13:1596–1608. [PubMed: 13678590]
32. Hirota T, Gerlich D, Koch B, Ellenberg J, Peters JM. Distinct functions of condensin I and II in mitotic chromosome assembly. J Cell Sci. 2004; 117:6435–6445. [PubMed: 15572404]
33. Renshaw MJ, et al. Condensins promote chromosome recoiling during early anaphase to complete sister chromatid separation. Dev Cell. 2010; 19:232–244. [PubMed: 20708586]
34. Charbin A, Bouchoux C, Uhlmann F. Condensin aids sister chromatid decatenation by topoisomerase II. Nucleic Acids Res. 2014; 42:340–348. [PubMed: 24062159]
35. Poirier M, Eroglu S, Chatenay D, Marko JF. Reversible and irreversible unfolding of mitotic newt chromosomes by applied force. Mol Biol Cell. 2000; 11:269–276. [PubMed: 10637307]
36. Cuylen S, Metz J, Haering CH. Condensin structures chromosomal DNA through topological links. Nat Struct Mol Biol. 2011; 18:894–901. [PubMed: 21765419]
37. Shintomi K, Hirano T. The relative ratio of condensin I to II determines chromosome shapes. Genes Dev. 2011; 25:1464–1469. [PubMed: 21715560]
38. Fujiwara T, Tanaka K, Kuroiwa T, Hirano T. Spatiotemporal dynamics of condensins I and II: evolutionary insights from the primitive red alga Cyanidioschyzon merolae. Mol Biol Cell. 2013; 24:2515–2527. [PubMed: 23783031]
39. Burmann F, et al. An asymmetric SMC-kleisin bridge in prokaryotic condensin. Nat Struct Mol Biol. 2013; 20:371–379. [PubMed: 23353789]
40. Cuylen S, Metz J, Hruby A, Haering CH. Entrapment of chromosomes by condensin rings prevents their breakage during cytokinesis. Dev Cell. 2013; 27:469–478. [PubMed: 24286828]
41. Oliveira RA, Hamilton RS, Pauli A, Davis I, Nasmyth K. Cohesin cleavage and Cdk inhibition trigger formation of daughter nuclei. Nat Cell Biol. 2010; 12:185–192. [PubMed: 20081838]
42. Nagy, A.; Gertsenstein, M.; Vintersten, K.; Behringer, R. Manipulating the Mouse Embryo A Laboratory Manual. 3rd edn. Cold Spring Harbor Laboratory Press: 2003.
43. Kitajima TS, Ohsugi M, Ellenberg J. Complete kinetochore tracking reveals error-prone homologous chromosome biorientation in mammalian oocytes. Cell. 2011; 146:568–581. [PubMed: 21854982]
44. Rattani A, et al. Sgol2 provides a regulatory platform that coordinates essential cell cycle processes during meiosis I in oocytes. eLife. 2013; 2:e01133. [PubMed: 24192037]

Europe PMC Funders Author Manuscripts

Europe PMC Funders Author Manuscripts

a

	NCAPH1	NCAPH2
Deletion efficiency ♀ *flox*/+, ZP3-Cre x ♂ wild type	100% efficient *61 pups* : *28 +/+, 33 Δ/+*	100% efficient *92 pups* : *52 +/+, 40 Δ/+*
Fertility ♀ *flox/flox*, ZP3-Cre x ♂ wild type	Fertile *3* ♀ : *6* litters (*7, 7, 8, 9, 7, 7*)	Infertile *3*♀ : *no progeny*
Viability ♀Δ/+ × ♂Δ/+	No Δ/Δ born	No Δ/Δ born

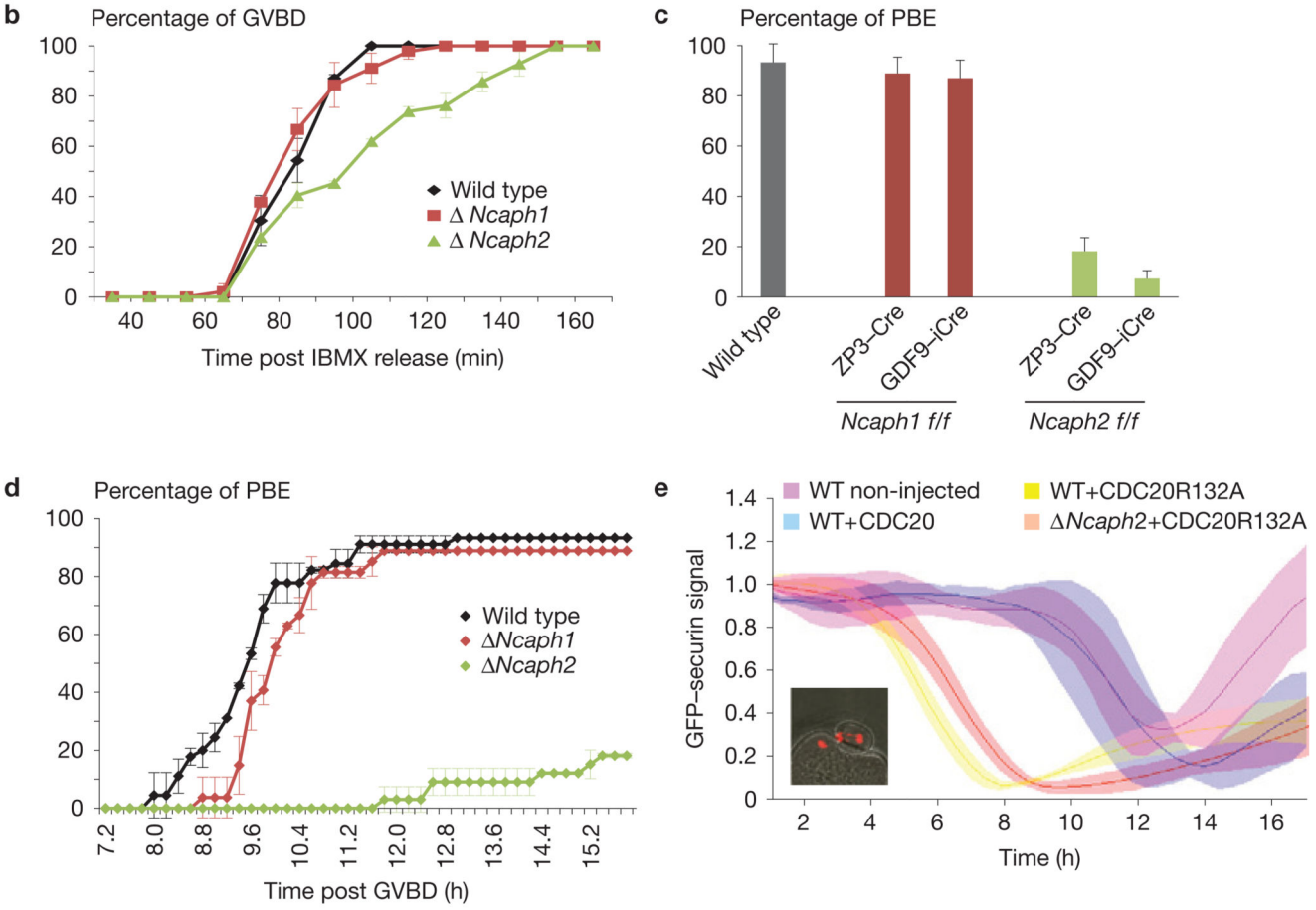

Figure 1.

Condensin II but not condensin I is essential for meiosis. (**a**) *Ncaph1*$^{fl/+}$ and *Ncaph2*$^{fl/+}$ mice were crossed as indicated to address three different questions: the deletion efficiency of ZP3Cre on the respective *flox* allele, the fertility of *Ncaph1*$^{f/f}$ *Tg(ZP3Cre)* and *Ncaph2*$^{f/f}$ *Tg(ZP3Cre)* females, and the viability of the homozygous mice (Δ/Δ; 5 litters of 3 breeding pairs were analysed). In each case, three breeding pairs were analysed independently. (**b**) GVBD kinetics of wild-type, ΔNcaph1 and ΔNcaph2 oocytes. Oocytes were isolated in M16 supplemented with IBMX, after which IBXM was washed out and oocytes were followed by live cell confocal microscopy. The total number of oocytes are WT: $n = 46$, *Ncaph1*$^{f/f}$ *Tg(ZP3Cre)*: $n = 45$ and *Ncaph2*$^{f/f}$ *Tg(ZP3Cre)*: $n = 42$. Error bars represent mean ± s.d. (**c**) PBE efficiencies counted after 16 h of culture *in vitro*. The total number of oocytes are WT:

Europe PMC Funders Author Manuscripts

Europe PMC Funders Author Manuscripts

n = 46, *Ncaph1*$^{f/f}$ *Tg(ZP3Cre)*: *n* = 45, *Ncaph2*$^{f/f}$ *Tg(ZP3Cre)*: *n* = 42, *Ncaph1*$^{f/f}$ *Tg(Gdf9–iCre)*: *n* = 35 and *Ncaph2*$^{f/f}$ *Tg(Gdf9–iCre)*: *n* = 112. Error bars represent mean ± s.d. (**d**) PBE kinetics of oocytes followed by live cell confocal microscopy. The total number of oocytes are WT: *n* = 46, *Ncaph1*$^{f/f}$ *Tg(ZP3Cre)*: *n* = 45 and *Ncaph2*$^{f/f}$ *Tg(ZP3Cre)*: *n* = 42. Error bars represent mean ± s.d. (**e**) The lack of PBE in *Ncaph2*$^{flox/flox}$ *Tg(Zp3Cre)* oocytes and SAC activation. Oocytes were injected at the GV stage with RNA coding for securin–eGFP and wild-type CDC20 or CDC20R132A mutant. The degradation of securin–eGFP was monitored by low-resolution live cell imaging and quantified. Values from individual oocytes were normalized relative to that at GVBD (0 h), and mean and standard deviations of the population are plotted in arbitrary units, (a.u.), against time. The CDC20R132A mutant induces PBE with massive segregation defects in Δ*Ncaph2* oocytes (inset). The total number of oocytes are WT: *n* = 5, WT+CDC20: *n* = 6, WT+CDC20R132A: *n* = 6, *Ncaph2*$^{f/f}$ *Tg(ZP3Cre)*+CDC20: *n* = 7. In **b**,**d**, oocytes were collected from one female of each genotype per experiment in three independent experiments. In **c**, oocytes were collected from one or two females of each genotype per experiment in three independent experiments. In **e**, oocytes were collected from one female of each genotype per experiment in two independent experiments.

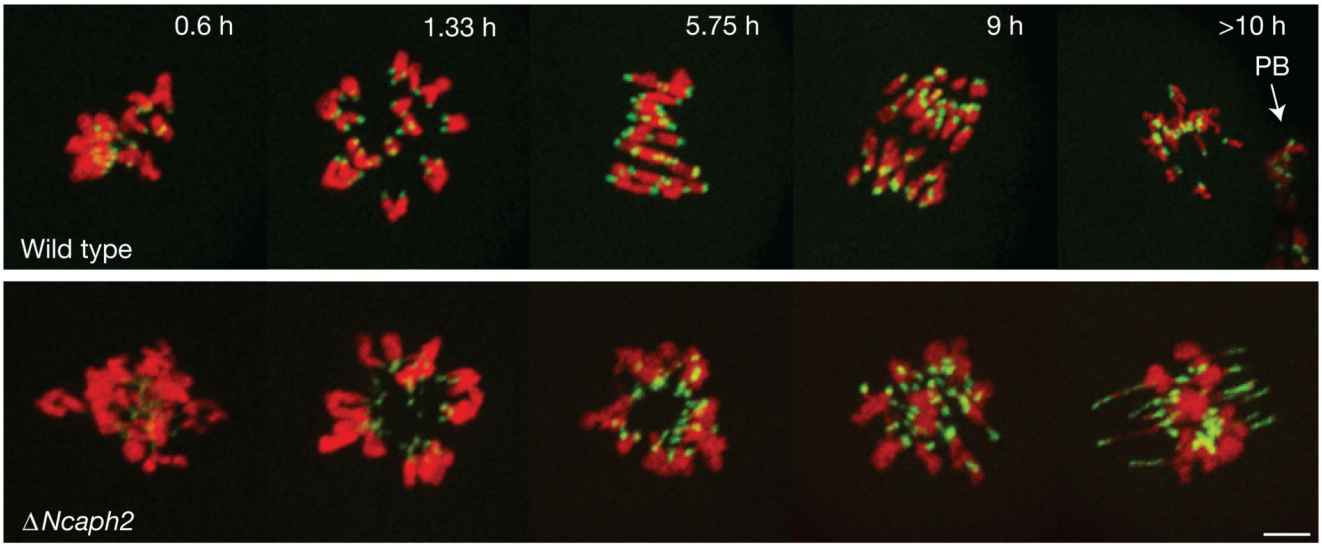

Figure 2.

Condensin II determines the morphology and rigidity of meiotic bivalents. Oocytes from *Ncaph2*$^{f/f}$ females (wild-type *Ncaph2*) or *Ncaph2*$^{f/f}$ *Tg(ZP3Cre)* females (Δ*Ncaph2)* were injected at the GV stage with mRNA coding for H2B–mCherry to mark the whole chromosomes in red and TALE-mClover_MajSat to mark the pericentric repeats in green. Meiosis I progression was followed by live cell confocal imaging. Maximum intensity *z* projection images of the main time points are shown between 0.6 h post-GVBD and more than 10 h after, when the polar body (PB) is extruded by the wild-type control. The phenotype was observed in all oocytes analysed (oocyte number >50, female number >5, more than three experiments). Scale bar, 5 μm.

Europe PMC Funders Author Manuscripts
Europe PMC Funders Author Manuscripts

Europe PMC Funders Author Manuscripts

Europe PMC Funders Author Manuscripts

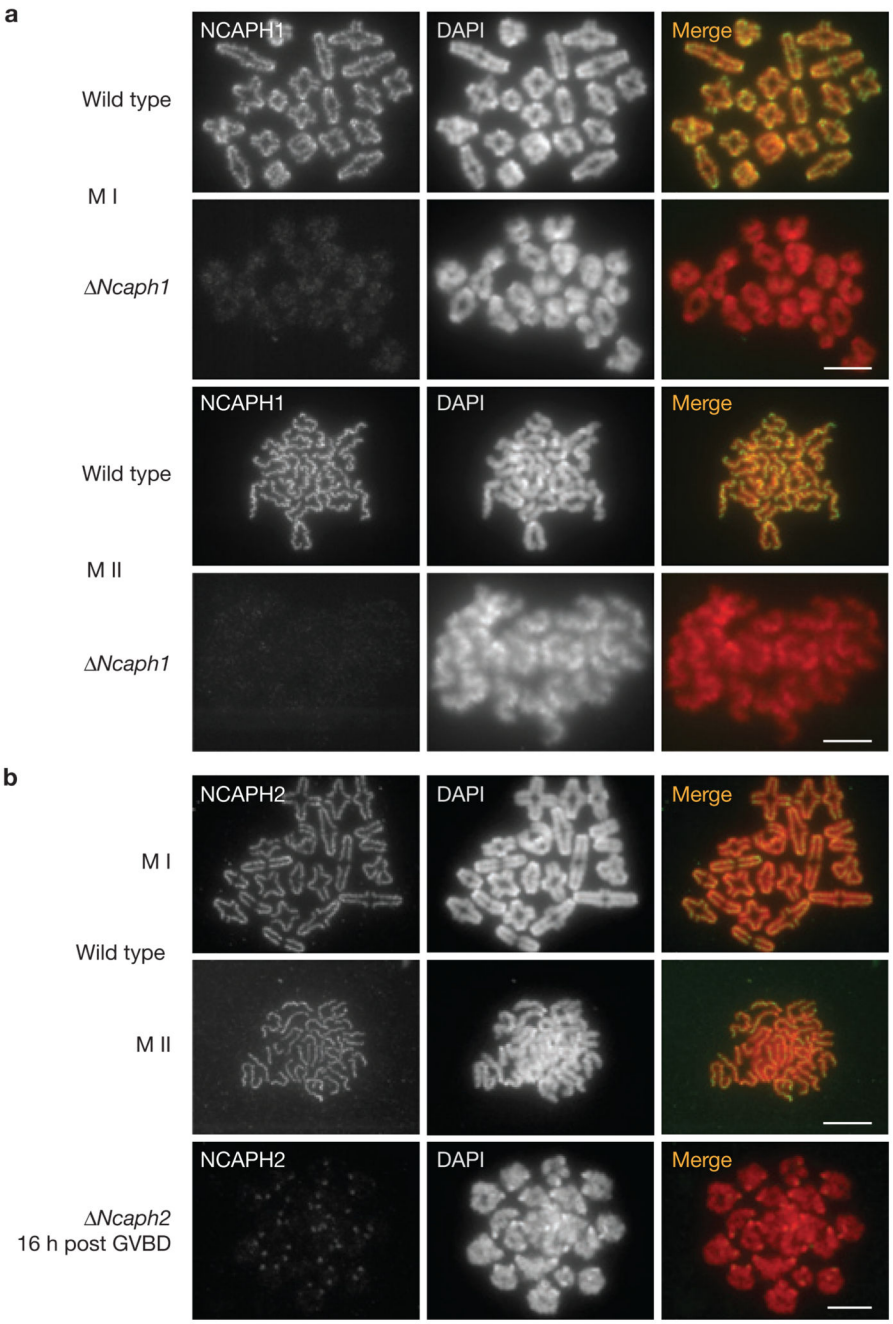

Figure 3.

Deletion of Ncaph1 or Ncaph2 induces different condensation defects. (**a**,**b**) Chromosomes from oocytes isolated from *Ncaph1*$^{f/f}$ *Tg(ZP3Cre) (ΔNcaph1)* (**a**) or *Ncaph2*$^{f/f}$ *Tg(ZP3Cre) (ΔNcaph2)* (**b**) females were analysed by chromosome spreading 7 h (meiosis I) or 16 h (meiosis II) after GVBD. The depletion levels were analysed by immunofluorescence using antibodies directed against NCAPH1 or NCAPH2. The DNA was stained with DAPI. Oocytes from *Ncaph1*$^{f/f}$ or *Ncaph2*$^{f/f}$ females were used as the control (wild type). As 80% of Δ*Ncaph2* oocytes do not extrude the polar body, stretched bivalents are observed 16 h

post-GVBD. The phenotypes were observed in all oocytes analysed (oocyte number >20, female number >5, more than three experiments). Scale bars, 5 μm.

Europe PMC Funders Author Manuscripts

Europe PMC Funders Author Manuscripts

Europe PMC Funders Author Manuscripts

Europe PMC Funders Author Manuscripts

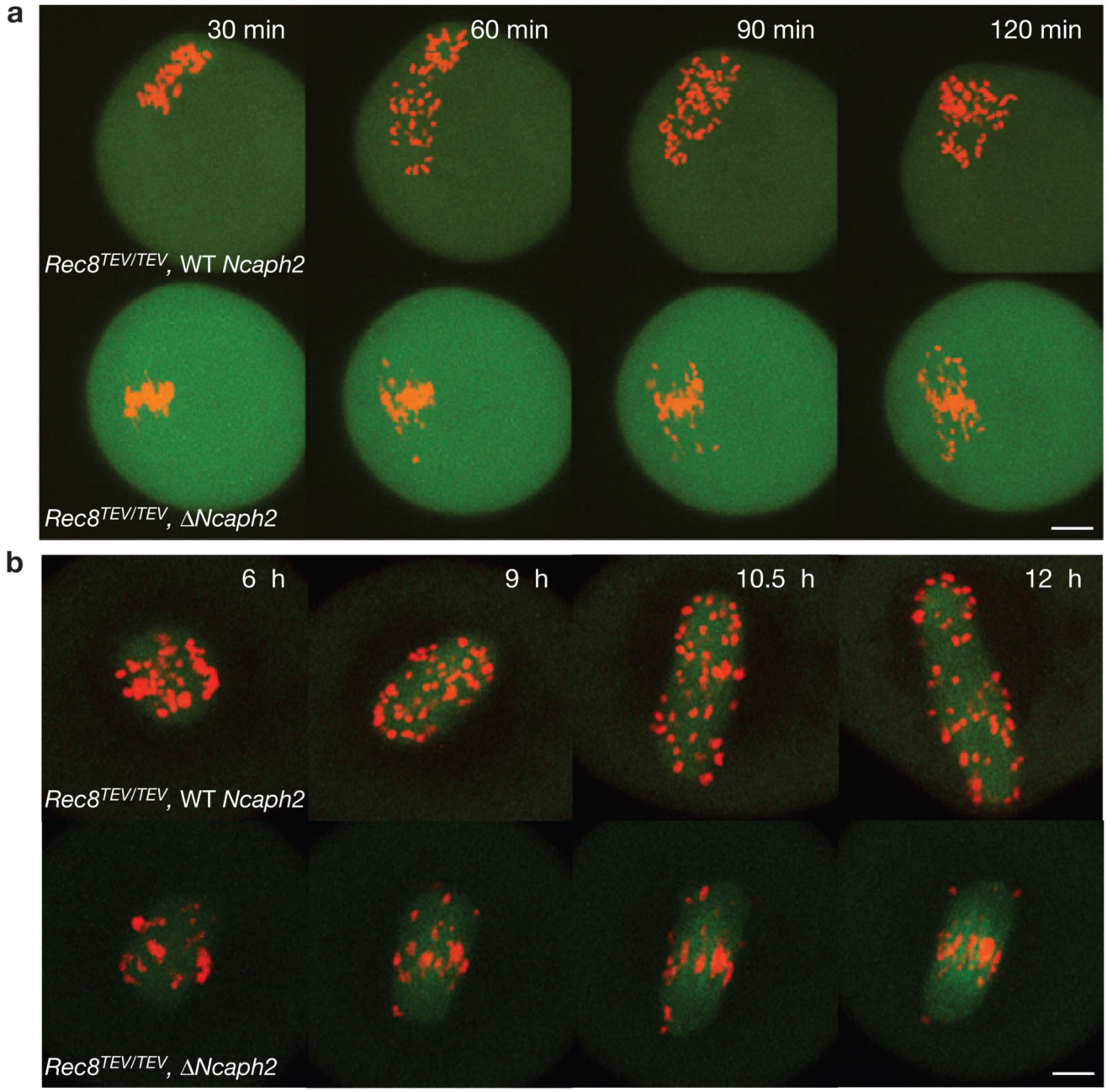

Figure 4.

Condensin is required for sister chromatid disentanglement even in the absence of cohesin. (**a**) Oocytes from *Rec8*$^{TEV/TEV}$ *Ncaph2*$^{f/f}$ *(Rec8*$^{TEV/TEV}$, WT *Ncaph2)* or *Rec8*$^{TEV/TEV}$, *Ncaph2*$^{f/f}$ *Tg(ZP3Cre) (Rec8*$^{TEV/TEV}$, Δ*Ncaph2)* females were injected at the GV stage with H2B–mCherry, securin–eGFP and Mad2 mRNA. Sixteen hours after GVBD, the oocytes arrested in metaphase I owing to MAD2 overexpression were injected with TEV protease mRNA and chromosomes were followed by live cell confocal imaging. Maximum-intensity *z* projection images of the indicated time points post TEV injection are shown. The phenotype was observed in all oocytes analysed (oocyte number = 15, female number 3,

three experiments). (**b**) Oocytes from *Rec8*$^{TEV/TEV}$ *Ncaph2*$^{f/f}$ *(Rec8*$^{TEV/TEV}$, WT *Ncaph2)* or *Rec8*$^{TEV/TEV}$, *Ncaph2*$^{f/f}$ *Tg(ZP3Cre) (Rec8*$^{TEV/TEV}$, Δ*Ncaph2)* females were injected at the GV stage with mRNA coding for H2B–mCherry, eGFP–tubulin and TEV protease. Chromosomes were followed by live cell confocal imaging. Maximum-intensity *z* projection images of the indicated time points post-GVBD are shown. The phenotype was observed in all oocytes analysed (oocyte number = 19, female number = 3, three experiments). Scale bars, 10 μm.

Europe PMC Funders Author Manuscripts

Europe PMC Funders Author Manuscripts

Europe PMC Funders Author Manuscripts

Europe PMC Funders Author Manuscripts

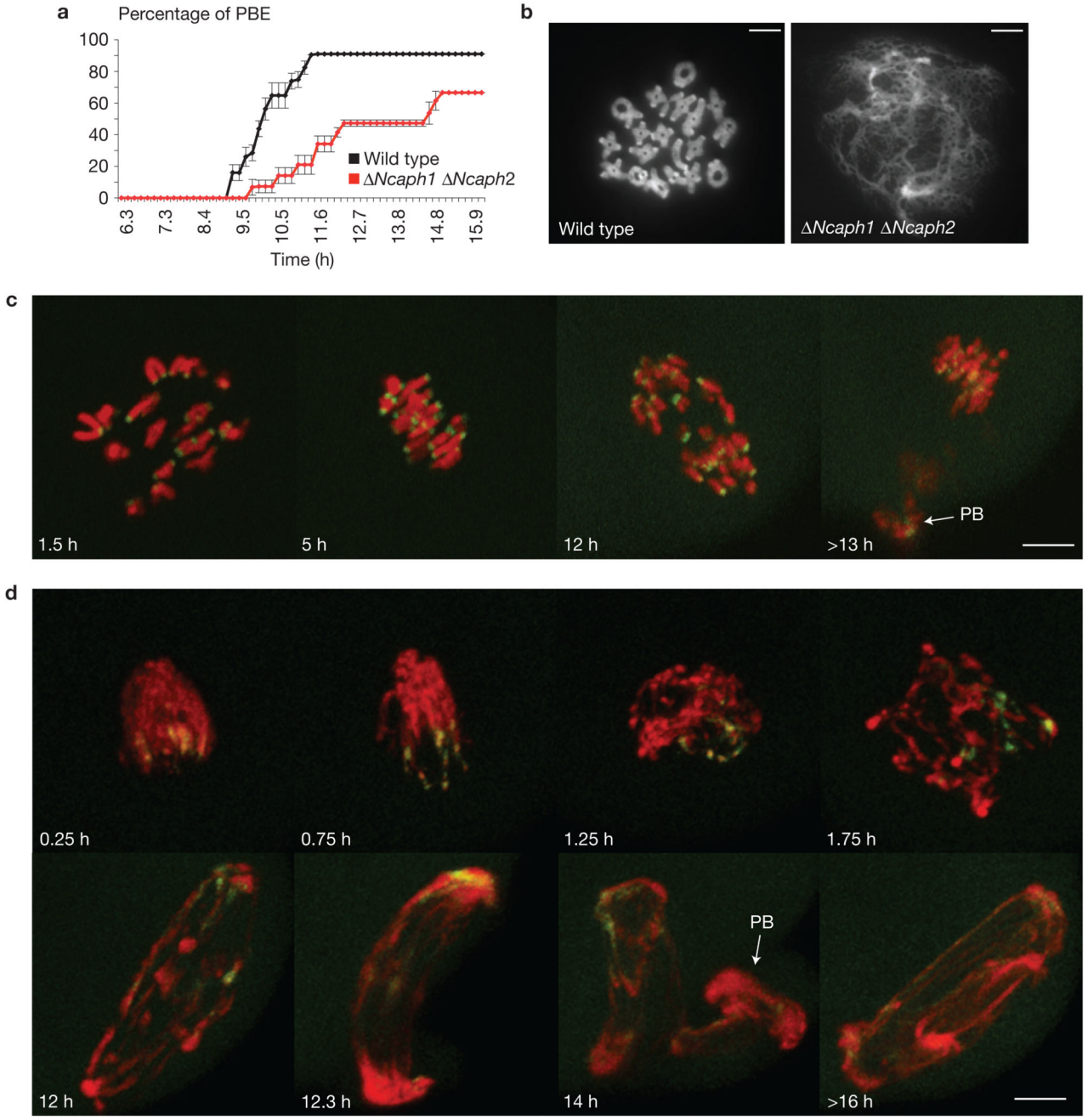

Figure 5.

Condensins I and II have overlapping functions. (**a**) PBE kinetics of oocytes isolated from females *Ncaph1*$^{f/f}$ *Ncaph2*$^{f/f}$ *Tg(ZP3Cre)*. Oocytes from littermate *Ncaph1*$^{f/f}$ *Ncaph2*$^{f/f}$ females were used as the control. The two groups of oocytes were followed by live cell confocal microscopy to evaluate the time post-GVBD at which the polar body was extruded. Results are from two independent experiments realized using oocytes from one female of each genotype per experiment. The total number of oocytes are *Ncaph1*$^{f/f}$ *Ncaph2*$^{f/f}$: $n = 11$ and *Ncaph1*$^{f/f}$ *Ncaph2*$^{f/f}$ *Tg(ZP3Cre)*: $n = 15$. Error bars represent mean ± s.d. (**b**)

Chromosome spreading 7 h post-GVBD of wild-type and Δ*Ncaph1* Δ*Ncaph2* oocytes stained with DAPI. The phenotype was observed in all oocytes analysed (oocyte number = 18, female number = 3, three experiments). Scale bar, 5 μm. (**c**,**d**). Oocytes from *Ncaph1*$^{f/f}$ *Ncaph2*$^{f/f}$ females (top) or *Ncaph1*$^{f/f}$ *Ncaph2*$^{f/f}$ *Tg(ZP3Cre)* females (bottom) were injected at the GV stage with mRNA coding for H2B–mCherry and TALE-mClover_MajSat. Meiosis I progression was followed by live cell confocal imaging. Maximum-intensity *z* projection images of the main time points are shown (PB, polar body). The phenotype was observed in all oocytes analysed (oocyte number = 32, female number = 3, three experiments). Scale bars, 7 μm.

Europe PMC Funders Author Manuscripts

Europe PMC Funders Author Manuscripts

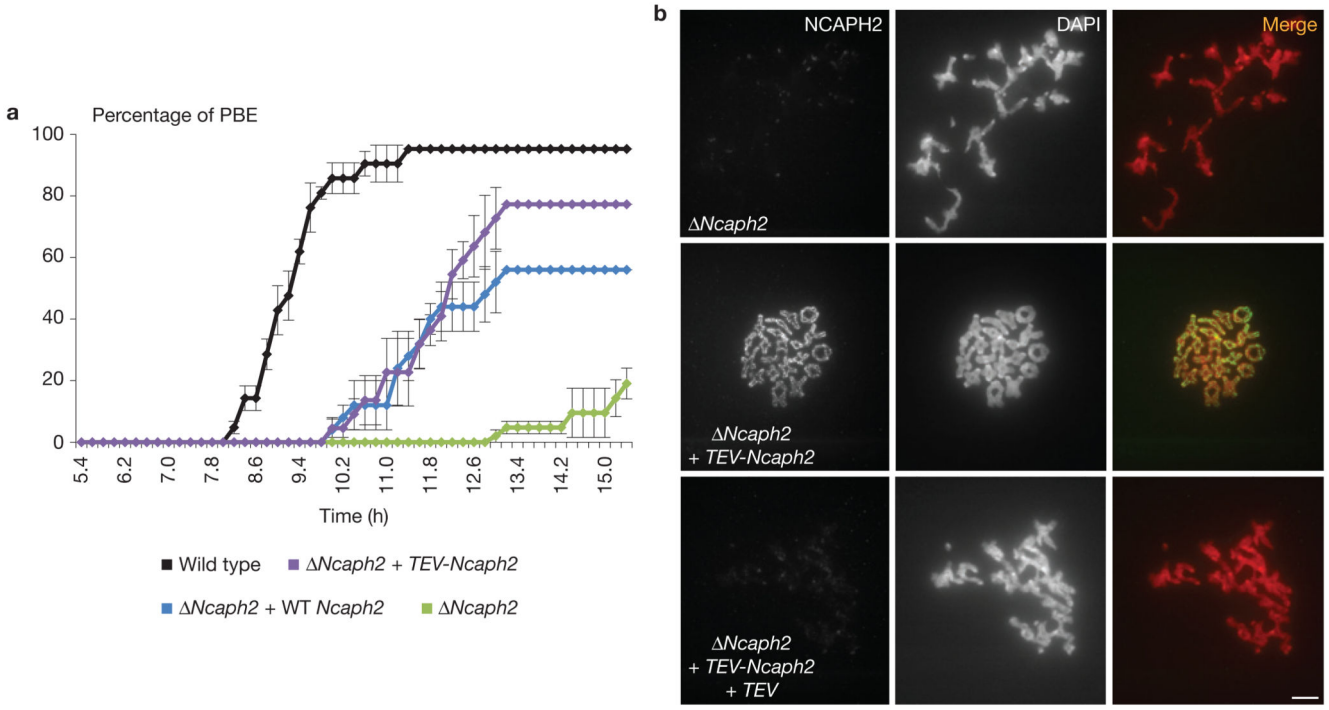

Figure 6.

Creation of a functional TEV-cleavable Ncaph2. (**a**) Oocytes were isolated from *Ncaph2*$^{f/f}$ *or Ncaph2*$^{f/f}$ *Tg(ZP3Cre)* females and injected at the GV stage with mRNA coding only for H2B–mCherry for wild type and Δ*Ncaph2*. Two groups of Δ*Ncaph2* oocytes were injected with wild-type *Ncaph2* or TEV-cleavable *Ncaph2*. The four groups of oocytes were followed by live cell confocal microscopy to evaluate the time post-GVBD at which the polar body was extruded. Results are from two independent experiments realized using oocytes from one female of each genotype per experiment. The total number of oocytes are wild type: n = 21, Δ*Ncaph2*: n = 23, Δ*Ncaph2* + wild-type *Ncaph2*: n = 22, Δ*Ncaph2* + TEV-cleavable *Ncaph2* n = 22. Error bars represent mean ± s.d. (**b**) Δ*Ncaph2* oocytes were injected at the GV stage with H2B–mCherry, H2B–mCherry + TEV-Ncaph2 or H2B–mCherry + TEV-Ncaph2 + TEV protease mRNA. Seven hours post-GVBD, chromosome spread analysis reveals that TEV-NCAPH2 is present on the chromosome scaffold (NCAPH2 immunostaining) and rescues the defects of chromosome organization (DAPI). However, no rescue is observed if the TEV protease-coding mRNA is co-injected. The phenotype was observed in all oocytes analysed (oocyte number = 10, female number = 2, two experiments). Scale bar, 5 μm.

Europe PMC Funders Author Manuscripts
Europe PMC Funders Author Manuscripts

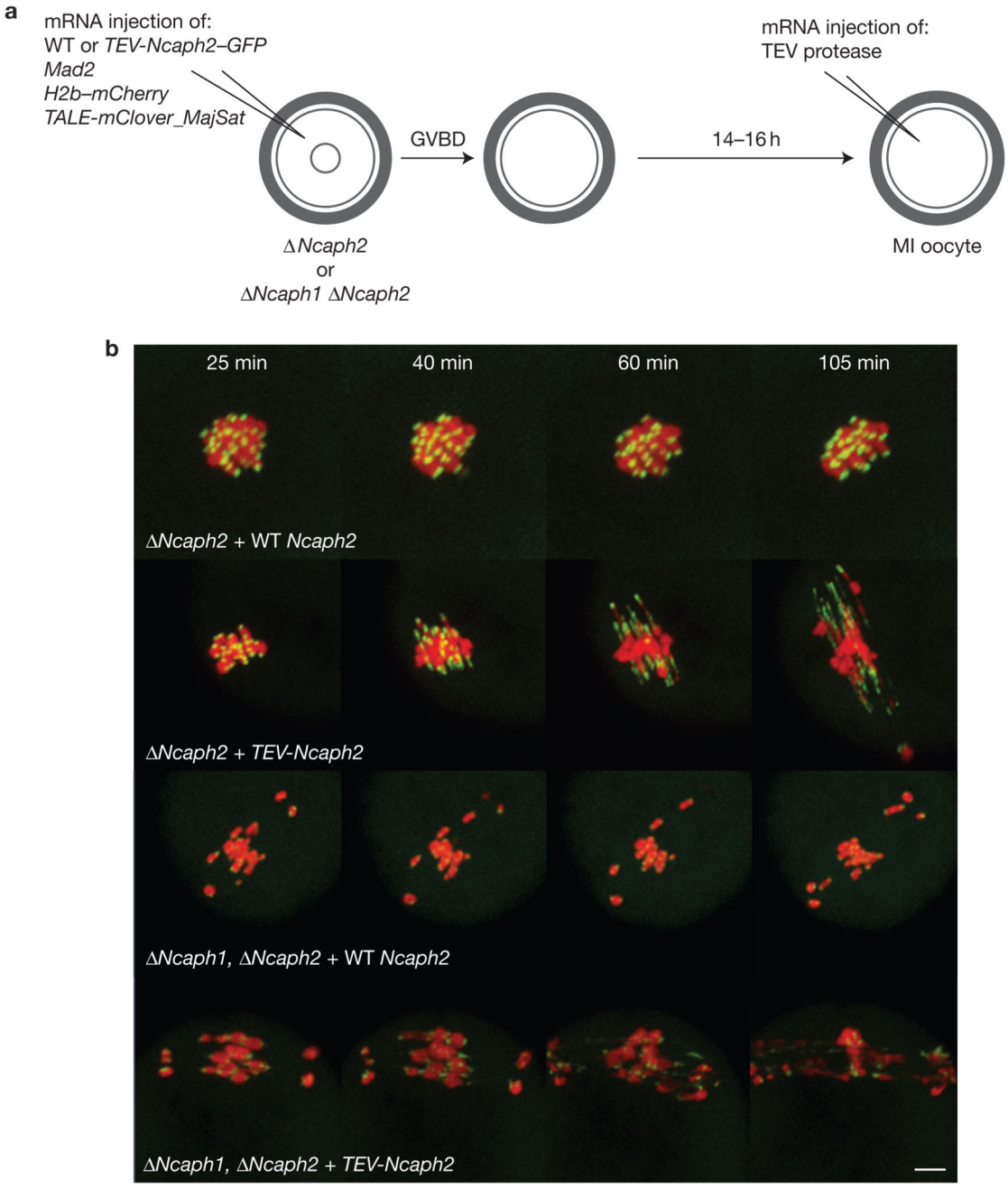

Figure 7.

Condensin maintains the morphology and rigidity of chromosomes. (**a**) Cartoon summarizing the experimental procedure. (**b**) Single *Ncaph2* mutant (*Ncaph2*$^{f/f}$ *Tg(ZP3Cre)*, top panel) or double mutant oocytes (*Ncaph1*$^{f/f}$ *Ncaph2*$^{f/f}$ *Tg(ZP3Cre)*, bottom panel) were injected at the GV stage with H2B–mCherry, TALE-mClover_MajSat, Mad2 and wild-type or TEV-cleavable NCAPH2. Sixteen hours after GVBD, the rescued oocytes arrested in metaphase I owing to MAD2 overexpression were injected with TEV protease mRNA and chromosomes were followed by live cell confocal imaging. Maximum-intensity *z* projection

Europe PMC Funders Author Manuscripts
Europe PMC Funders Author Manuscripts

images of the indicated time points post TEV injection are shown. The phenotypes were observed in all oocytes analysed in three independent experiments: $n > 15$ for each category. Scale bar, 5 μm.

Europe PMC Funders Author Manuscripts

Europe PMC Funders Author Manuscripts

Europe PMC Funders Author Manuscripts

Europe PMC Funders Author Manuscripts

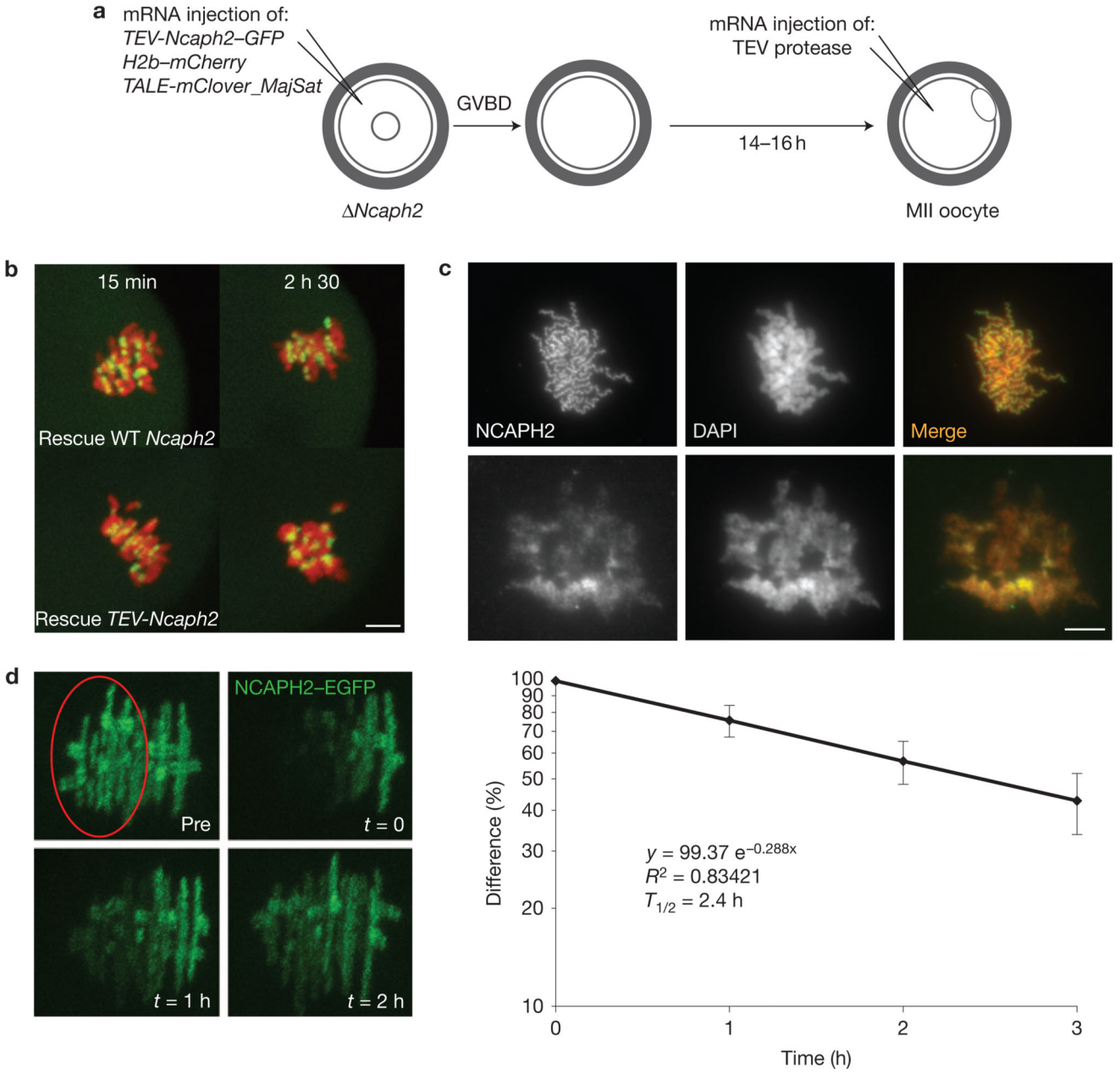

Figure 8.

The stable association of condensin II with chromosomes maintains their structure. (**a**) Cartoon representing the experimental procedure. (**b**) Single *Ncaph2* mutant oocytes were injected at the GV stage with H2B–mCherry, TALE-mClover_MajSat and wild-type or TEV-cleavable NCAPH2. Sixteen hours after GVBD, the rescued oocytes, naturally arrested in metaphase II were injected with TEV protease-coding mRNA and chromosomes were followed by live cell confocal imaging. Maximum-intensity *z* projection images of the indicated time points post TEV mRNA injection are shown. The phenotype was observed in all oocytes analysed (oocyte number >12, female number = 3, three experiments). Scale bar, 5 μm. (**c**) Chromosome spreads of the two different groups of oocytes, 2.5 h after TEV

Europe PMC Funders Author Manuscripts

Europe PMC Funders Author Manuscripts

mRNA injection, showing the disruption of chromosome structure after TEV-NCAPH2 cleavage (top: rescue WT Ncaph2, bottom: rescue TEV-Ncaph2). The phenotype was observed in all oocytes analysed (oocyte number = 12, female number = 2, two experiments). Scale bar, 5 μm. (**d**) Slow recovery of condensin II after photobleaching. *Ncaph2* oocytes were injected at the GV stage with H2B–mCherry-, MAD2- and NCAPH2–eGFP-coding mRNAs. After 16 h, half of the metaphase 1 chromosomes were photobleached (red circle) and the recovery of the eGFP signal was followed every hour. In the right panel, the average difference in mean eGFP fluorescence between bleached and non-bleached regions is plotted on a logarithmic scale (one experiment, $n = 11$ oocytes from two females). The trend line equation and the corresponding regression coefficient (R^2) were obtained using Microsoft Excel software: $y = y_0 * e^{-kx}$. The half-life of the protein on the chromosome was calculated using the equation: $T_{1/2} = \mathrm{Ln}(2)/k$. Error bars represent s.d.